Sensors & Actuators: B. Chemical 433 (2025) 137546

Contents lists available at ScienceDirect

Sensors and Actuators: B. Chemical

journal homepage: www.elsevier.com/locate/snb

A radiation toxicity biosensing platform based on radioresistant bacteria modified with *dr_0423*

Xin Cui [a,1], Chengpeng Yang [b,1], Vincent W.T. Li [b,1], Siping Huang [b], Xin Yao [c], Cia Hin Lau [b], Zhongning Jiang [b], Yun Qu [b], Marcos [c], Peter K.N. Yu [d], S.H. Cheng [e], Raymond H.W. Lam [b,f,*]

[a] *Key Laboratory of Biomaterials of Guangdong Higher Education Institutes, Department of Biomedical Engineering, Jinan University, Guangzhou, China*
[b] *Department of Biomedical Engineering, City University of Hong Kong, Hong Kong, China*
[c] *School of Mechanical and Aerospace Engineering, Nanyang Technological University, Singapore*
[d] *Department of Physics, City University of Hong Kong, Hong Kong, China*
[e] *Department of Biomedical Sciences, City University of Hong Kong, Hong Kong, China*
[f] *City University of Hong Kong Shenzhen Research Institute, Shenzhen, China*

ARTICLE INFO

Keywords:
Radiation toxicity
dr_0423
Whole-cell biosensor
Amperometric detection
Microfluidics

ABSTRACT

Radiation toxicity is important for evaluating potential health risks associated with radioactive substances or environmental radioactivity. Whole-cell biosensors can be applied to quantify radiation toxicity, yet it is technically challenging to identify a radiation-sensitive gene in a radioresistant strain and to maintain an ideal microenvironment for the promising radiation toxicity measurement. Herein, we report a microfluidic radiation toxicity whole-cell biosensing scheme based on a transgenic bacteria, membrane microfabrication, dielectrophoresis (DEP)-based cell trapping and amperometric detection. We have identified a radiation-responsive gene promoter (*dr_0423*) unique to the radioresistant strain *D. radiodurans*, leading to the development of transgenic bacteria *DRPZ423*. The *dr_0423* promoter activates the expression of beta-galactosidase upon DNA damage from ionizing irradiation, which catalyzes the conversion of *p*-aminophenyl beta-D-galacto-pyranoside (PAPG) to *p*-aminophenol (PAP), and generates electrons for amperometric detection. Our biosensing scheme was validated using X-ray and alpha particles, showing promising results with a relative standard deviation of 2.78–6.38 % and a recovery rate exceeding 93.3 %. This biosensing platform offers a reliable method for measuring radiation toxicity, suitable for various applications such as environmental hazard assessment and beyond.

1. Introduction

Over the past decades, radioactive waste has rapidly increased due to nuclear reactions, power generation, mining, and medical/scientific research [1,2]. In the U.S. alone, radioactive waste production is projected to grow from 47,000 tonnes in 2003 to 105,000 tonnes by 2035 [3–5]. Radioactive waste emits ionizing radiation (alpha, beta, gamma, and X-rays), which can damage DNA and lead to health issues such as cancer and reproductive failure [6]. Different radiation types cause varying levels of damage, with the International Commission on Radiological Protection (ICRP) assigning weighting factors to measure biological effectiveness: 1 for X-rays/gamma rays, 2 for protons, 2–20 for neutrons, and 20 for alpha radiation [7]. Improper handling of radioactive materials can result in environmental contamination and severe public health risks, especially as some countries have approved direct discharge of radioactive waste into oceans and urban wastewater systems [8,9]. Therefore, promising measurement of radioactive biotoxicity in the commercial products and the environment is a crucial line of defence for human health and safety.

Traditional radiation detection technologies include ionization chambers [2,10], proportional counters, Geiger-Muller counters [11], MOSFET dosimeters [12], and scintillation counters [2]. Advanced systems use commercial silicon photomultipliers and solid-state avalanche photodiodes for real-time beta-particle detection [13,14]. Cerenkov radiation imaging has also been used to quantify beta particle doses [15]. However, these methods exhibit varying sensitivities

* Corresponding author at: Department of Biomedical Engineering, City University of Hong Kong, Hong Kong, China.
E-mail address: rhwlam@cityu.edu.hk (R.H.W. Lam).
[1] Authors equally contributed.

https://doi.org/10.1016/j.snb.2025.137546
Received 6 September 2024; Received in revised form 27 February 2025; Accepted 28 February 2025

depending on the radiation types, as demonstrated by assays like the alkaline comet assay, with sensitivity ratios of ~1:1.5:2.5 for gamma, X-ray, and alpha particles, respectively [16]. Zinc oxide sensors, for example, show a ratio of 1:100 for X-rays and alpha particles [17]. Hence, these physical sensing methods face technical challenges in reliably showing the biotoxicity (*e.g.*, DNA damage in cells) caused by ionizing radiation, especially given that the radiation types are unknown in a test sample. Many of these methods also require a volume of radiation particles beyond the level present in many hazard samples [18, 19].

Engineered microorganisms offer an alternative method for detecting toxic-induced biotoxicity [20,21], responding to toxic materials including ionizing radiation with measurable optical [22,23] and electrochemical signals [24,25]. Unlike physical sensors, these 'toxicity biosensors' measure biotoxicity, reflecting DNA damage rather than just physical parameters [26]. Examples include *Pseudomonas aeruginosa* with *recA-lux* for detecting ultraviolet radiation [27,28] and *Escherichia coli* (*E. coli*) containing *recA* and *luxCDABE* for quantifying the dose of gamma ray [29]. Nevertheless, exposure to ionizing radiation reduces the viability of most microorganisms and limits the repeated and long-term implementation, meaning that there is a significant demand for looking for a more radioresistant strain and its radiation-responsive gene. Besides, these bacteria require extensive operational procedures, including manipulation of samples and reagents.

Microfluidics technology has been applied to develop whole-cell detectors with an improved sensitivity and reduced required sample volume requirements [30]. Whole-cell microfluidic biosensors [31–34] have been developed for screening biohazards and pollutants, such as actinomycetes [35], phenylethylamine [36], and marine pollutants like copper and lead [37]. Bioluminescent *E. coli* reporters have even been used to detect ciprofloxacin in milk using smartphones [37]. For evaluating bio-radiation effect, a compact microfluidic cytometer was reported to quantify the fluorescent intensity of γ-H2AX, a biological dosimeter, in lymphocyte cells irradiated by ultraviolet lights [38]. Furthermore, dielectrophoresis (DEP)-based cell trapping can be applied in the whole-cell biosensors, significantly improving sensitivity compared to bulk assays by concentrating cells [39]. Overall, these microfluidics-based biosensors (Table S1) inherit the merits of low cost, rapid detection, precise sample handling and improved portability [35, 40], yet the application of radioresistant bacteria as microfluidic biosensors for evaluating the biotoxicity of ionizing radiation is lacking.

In this work, we developed a novel microfluidic radiation toxicity biosensing platform that utilizes a transgenic strain of radioresistant bacteria, *D. radiodurans* (*DRPZ423*), as the biosensor probe. *DRPZ423* is engineered to express beta-galactosidase in response to ionizing radiation. To enhance detection sensitivity, DEP-based cell trapping is employed to concentrate the bacterial population within the radiation exposure zone. A key innovation of our system as compared with previous studies [41] is the incorporation of an ultra-thin polydimethylsiloxane (PDMS) membrane, which ensures that the bacteria are securely held in the irradiation chamber while allowing a wide spectrum of ionizing radiation, including alpha particles, to penetrate with minimal energy loss. This design overcomes the limitations of traditional systems that struggle with energy attenuation or inadequate sensitivity and specificity to diverse radiation sources. As the irradiation dose increases, the beta-galactosidase produced by *DRPZ423* is measured using a novel 'amperometric detection' scheme. This scheme refers to the electrochemical detection method utilized to measure the enzymatic activity of beta-galactosidase, which catalyzes the conversion of *p*-aminophenyl beta-D-galacto-pyranoside (PAPG) to p-aminophenol (PAP), in which the generated electrical current is measured. This design enables precise detection of radiation toxicity from various doses of ionizing radiation, and operates using a small volume of radioactive samples, offering an efficient and sensitive electrochemical microfluidic platform for radiation toxicity assessment.

2. Results

2.1. Design and sensing principle of a radiation toxicity biosensing platform

To detect the genotoxicity of ionizing radiations, we developed a transgenic strain-embedded radiation toxicity biosensing platform with the microstructure configured based on the *in vivo* environment of human epithelial cells (Fig. 1**a**). Generally, the cell membrane is located at a distance from the cell nucleus with a typical distance of 5 – 10 μm for epithelial cells [42]. This can offer a natural barrier for protecting the DNA from ionizing radiations, which can penetrate through cell membrane and cytoplasm and cause DNA damage either directly by ionizing atoms of DNA molecules or indirectly by interaction with free radicals [43]. For example, the epithelial lining in human stomach constantly undergoes self-renewal, with rapid division and differentiation [44]. This high turnover rate can make stomach cells more susceptible to DNA damage when ingesting radioactive particle-contaminated substances [45]. Among various radiations, alpha radiation is the most difficult to detect because of its short range and weak penetration power [46], yet it can have a high ionizing capability and cause high genotoxicity to single cells.

A microfluidic biosensing device (Fig. 1b&c), designed to detect ionizing radiation, includes four key components: an ultra-thin PDMS membrane (1.5 μm thick) (Fig. 1b & Fig. S2&S3), an irradiation chamber, an electrochemical detection chamber, and genetically engineered *DRPZ423* bacteria. (The fabrication process is available in Supplementary Material.) This device has a 10 μm high, 100 μm wide flow channel, with a total length of ~6 cm. An inlet pressure of 0.1 kPa generates a flow rate of ~0.833 nl/min, aligning with our measurements. The inlet pressure is driven by a portable precise pressure pump (Elveflow AF1, 220 ×130 ×130 mm) and regulated by a custom microfluidic chip (Fig. S1). The membrane thickness has been controlled by spin coating the PDMS pre-polymer solution with its viscosity reduced by mixing with hexane (1:10 w/w). The ultra-thin membrane allows radiation to penetrate, while isolating other soluble factors, improving measurement specificity. Inside the irradiation chamber (Fig. 1b&c), DEP forces are applied to trap *DRPZ423* bacteria, focusing them near the radiation source to increase sensitivity [41,47]. Consistent with previous studies, the DEP-based bacteria trapper had two side electrodes (30 μm × 300 μm, centre-to-centre distance 1.17 mm) sandwiching a pair of trapping electrodes (200 μm × 300 μm, centre-to-centre distance 300 μm). Upon exposure to ionizing radiation, the bacteria express beta-galactosidase, driven by the radiation-responsive *dr_0423* promoter. This enzyme converts PAPG into PAP, which diffuses across the cell membrane and is carried into the detection chamber. In the electrochemical chamber (Fig. 1c&d), PAP is oxidized to p-quinone imine, and the current generated is measured using the amperometric detection (0.05 V applied), allowing for quantification of radiation toxicity (Fig. 1e). Moreover, the electrochemical detection chamber (Fig. 1c&d) has three electrodes: one reference electrode and two interconnected working electrodes containing multiple pairs of micro-fingers [41]. Each micro-finger was 600 μm long and 20 μm wide and with a gap of 20 μm between each other. The miniaturized electrode design can measure the local current across the microstructures, which is representative to irradiation responses of the trapped bacteria. The detailed operation procedures of the radiation toxicity biosening platform is described in Supplementary Material. Notably, the system is reusable, with fresh batches of *DRPZ423* cells, and requires only minimal radioactive material handling, eliminating the need for sophisticated equipment such as luminescence readers.

2.2. Screening of target genes sensitive to DNA damage upon radiation

We have investigated *D. radiodurans* to identify a defined plasmid capable of generating a measurable analytical signal responsive to

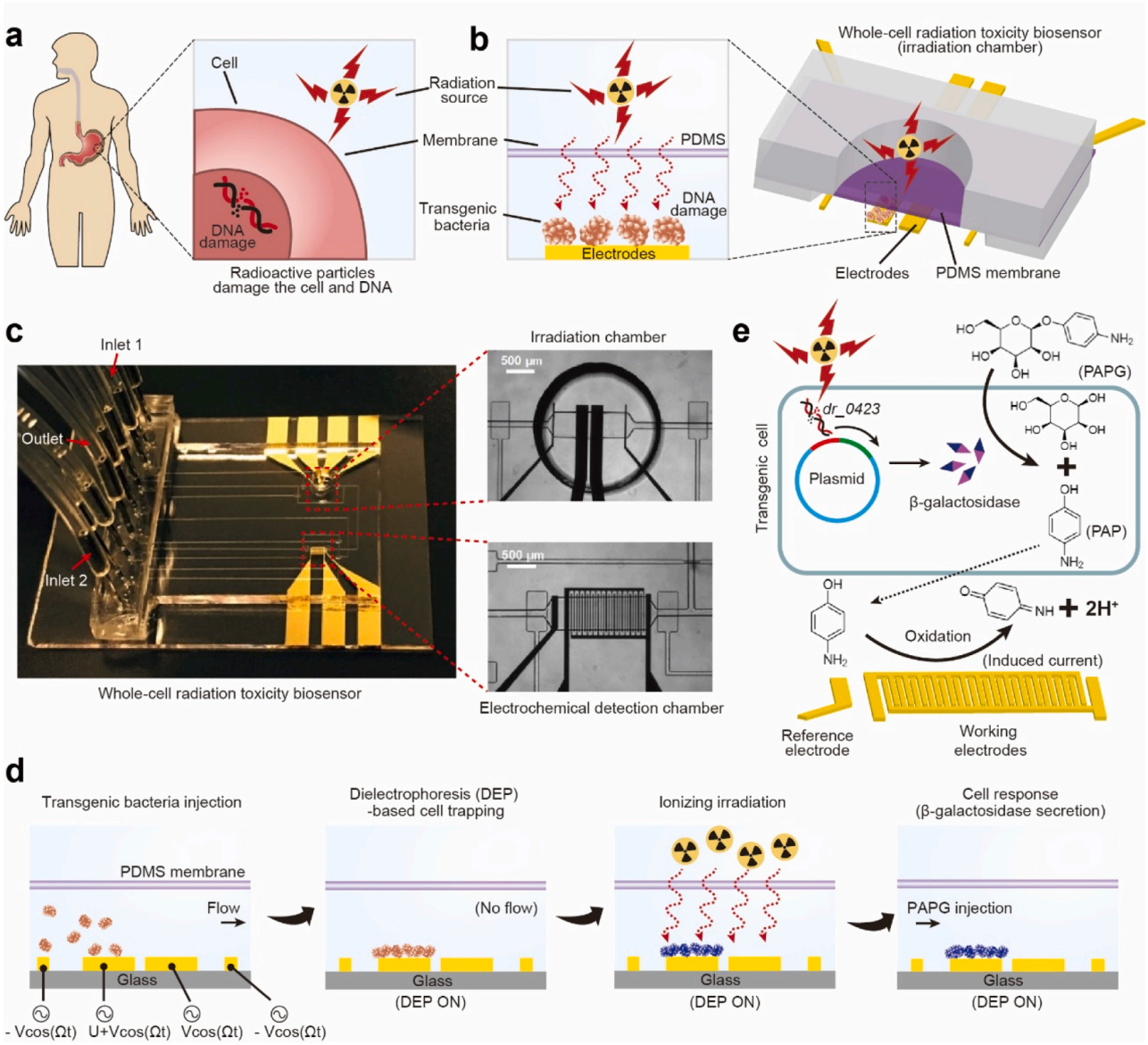

Fig. 1. Radiation toxicity biosensor using transgenic radioresistant bacteria. (a) Structure of an epithelial cell having multicompartment structures including cell membrane and cell nucleus. (b) Schematic of an ultra-thin PDMS membrane-separated, genetically engineered bacteria *DRPZ423*-based electrochemical microfluidic system for radiation toxicity detection inspired by the epithelial cell. (c) Representative images of the radiation toxicity biosensor, highlighting the DEP-based bacteria trapping unit and the electrochemical detection unit. Red arrows indicate the locations of Inlet 1, Inlet 2, and Outlet in the microfluidic chip. (d) Schematic of detection procedures of the radiation toxicity biosensor including genetically engineered bacteria *DRPZ423* loading, DEP-based cell trapping, on-chip cell radiation and injecting PAPG into the bacteria trapping chamber to electrochemically evaluate the radiation toxicity. (e) Principle of electrochemical detection.

ionizing irradiation. *D. radiodurans* has been chosen for more durable biosensing because of its well-known radiation-resistance contributed by the efficacious RecFOR-involved DNA repair system, unique ploidy genome structure and damaged DNA protection from degradation [48–50]. Noted, we also hypothesize that *D. radiodurans* contain gene regulatory elements such as gene promoters that correspond to the radiation-resistance and the underlying DNA repair mechanism triggered by radiation exposure. Discovery of such radiation-induced gene regulatory elements can lead to the construction of a more promising and durable biosensing element.

We screened the candidate genes involved in DNA damage, DNA repair and anti-oxidative stress mechanism and explored their sensitivity to irradiation. The genes *dr_0423* (DNA damage/repair responsive gene), *dr_0906* (DNA damage responsive gene), *dr_0944* (antioxidant responsive gene), *dr_1245* (DNA damage/repair responsive gene), *dr_1279* (antioxidant responsive gene), *dr_1546* (antioxidant responsive gene), *dr_1849* (antioxidant responsive gene), *dr_1913* (DNA damage responsive gene), *dr_1998* (antioxidant responsive gene), *dr_2085* (DNA repair responsive gene), *dr_A0145* (antioxidant responsive gene), *dr_A0259* (antioxidant responsive gene), and *dr_B0067* (antioxidant responsive gene) (Table S2) are chosen according to previous transcriptome dynamic studies [49,51,52]. mRNA expressions of the chosen genes in *D. radiodurans* upon irradiation were examined by real-time RT-PCR using *gap* as an internal reference [53], for the relative fold-changes of the gene expression level (Fig. 2a). As preliminary screening, *D. radiodurans* were first transferred to a 96-well plate and exposed to 100 ppm of sodium selenite (Sigma Aldrich, USA; at 30 °C for 1 h), an oxidative stress inducible agent to mimic the radiation toxicity [54]. Results (Fig. 2b) show that the expressions of *dr_0423*, *dr_1998*, *dr_1849* and *dr_2085* were significantly upregulated. We conducted further screening by applying X-ray irradiation (X-RAD 320 irradiator, Precision X-Ray Inc., North Branford, CT, USA) with different doses

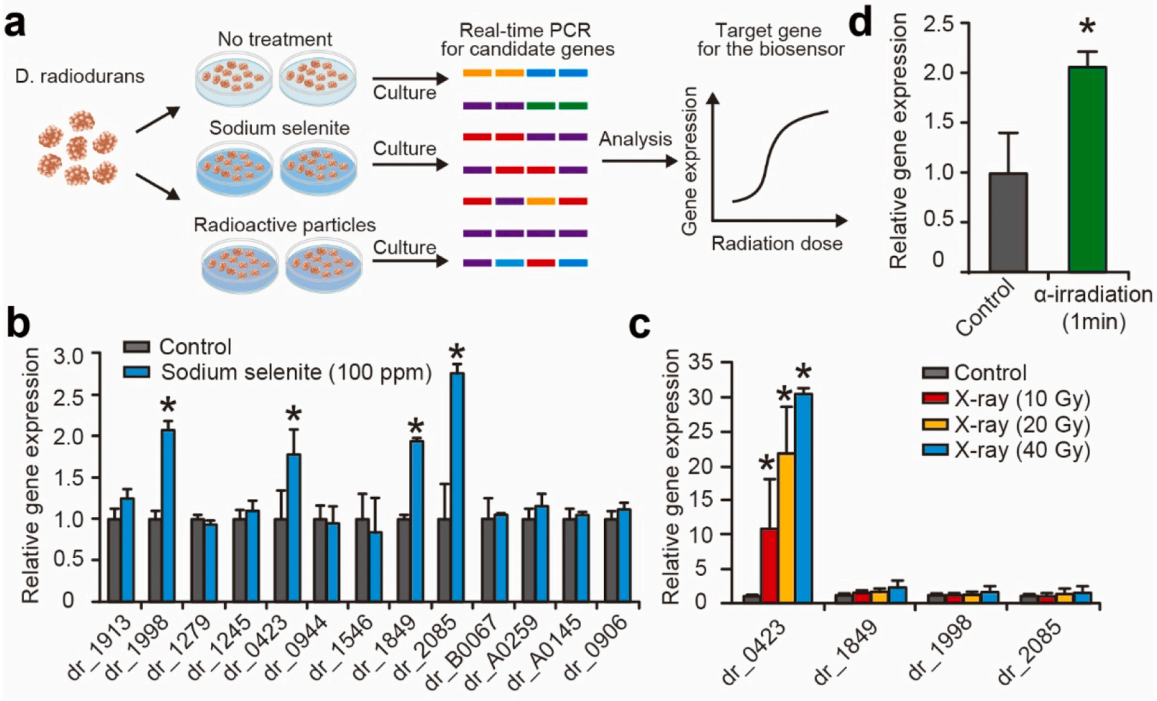

Fig. 2. Screening target genes sensitive to DNA damage upon radiation. (a) Schematic of the experiment design for screening target genes sensitive to DNA damage upon radiation in radiation-resistance *D. radiodurans* strain (wild-type). (b) Relative expression of various genes involved in DNA damage, DNA repair and anti-oxidative stress mechanism after sodium selenite (100 ppm) exposure (n = 3). (c) Relative expression of various genes with different doses (0 Gy, 10 Gy, 20 Gy and 40 Gy) of X-ray irradiation. Only *dr_0423* was found to be significantly upregulated (n = 3). (d) Relative expression of the *dr-0423* gene upon exposure to 1 min of alpha-particle irradiation using ^{241}Am isotopes (n = 6). Data are presented as mean ± SEM; and asterisks denote significant differences with p-values < 0.05.

(0 Gy, 10 Gy, 20 Gy and 40 Gy) and examined expressions of these four genes. Results demonstrate that only *dr_0423* was consistently upregulated by X-ray irradiation (Fig. 2c). To double confirm, we applied ^{241}Am isotopes to irradiate the bacteria with alpha particles and quantify for the *dr_0423* expression. Again, results (Fig. 2d) show that *dr_0423* was increased by about two-fold after 1 min of the alpha-particle irradiation. As *dr_0423* strongly responses to ionizing irradiation exposure, we cloned the gene promoter of *dr_0423* at the upstream of *lacZ* gene to track this gene promoter activity upon exposure to ionizing irradiation. Noteworthy, *dr_0423* is a unique gene in *D. radiodurans*. *dr_0423* is designated as a DNA damage responsive A gene (*DdrA*), which is a homologue of the eukaryotic Rad52 protein and can bind to both single-stranded and double-stranded DNA and protected the DNA from nucleolytic degradation after double strand break [55], thereby serves as an important role in genome restitution. Its expression is induced during the occurrence of DNA strand breaks, most probably through activation of its gene regulatory element (promoter) and/or a post-translational mechanism that reduces *DdrA* turnover. It has also been reported that a *dr_0423* mutant became more sensitive to the lethal effects of other DNA damage agents. For example, viability of *dr_0423*-mutated bacteria after exposure to ultraviolet and mictomycin C was decreased by as much as eight folds higher than that of the wild-type R1 strain [48], implying the prominent role of *dr_0423* in DNA damage repair.

2.3. Engineering transgenic strain DRPZ423 as a synthetic radiation sensing element

Beta-galactosidase acts as a reporter gene, cleaving lactose into galactose and glucose, which can be converted into various detectable signals (fluorescent, chemiluminescent, *etc.*) with a detection limit of 1.26×10^{-3} U/ml [56]. Inspired by this, we then engineered a plasmid containing *dr_0423*, *lacZ* (beta-galactosidase) and anti-chloramphenicol genes to correlate *dr_0423* regulatory activity with beta-galactosidase and chloramphenicol acetyltransferase (CAT) production. (The construction of the target recombinant plasmid and transgenic strain are described in Supplementary Material.)

As shown in Fig. 3a, we cloned the *dr_0423* gene promoter (P*dr_0423*) with two radiation/desiccation response motifs (RDRMs) via PCR. This was ligated with the *lacZ* operon from vector *PRADZ1* [57], generating the plasmid pRADZ-423. Using calcium chloride transformation, we introduced the plasmid into *D. radiodurans*, creating the transgenic strain *DRPZ423*, capable of producing beta-galactosidase and CAT in response to irradiation or DNA damage. Chloramphenicol screening (12.5 g/ml) was applied to confirm successful transformants. X-ray irradiation and a beta-galactosidase activity assay validated DRPZ423's function (Fig. 3b), with cells showing a lag phase of ~8 h and a doubling time of > 8 h (Fig. S4). The beta-galactosidase activity was measured using a commercial beta-galactosidase assay kit (Thermo Scientific, Rockford, IL) with the procedures as described in Supplementary Material. For better measurement consistency, the cells after a subculture of 5 – 8 h were used such that the cell growth was still in the lag phase such that the cell population could be roughly maintained.

We first measured the beta-galactosidase activity of *DRPZ423* and wild-type *D. radiodurans* following sodium selenite exposure for 60 min (Fig. 3c). The wild type produced no beta-galactosidase under selenite treatment, while *DRPZ423* showed a stronger beta-galactosidase activity with increasing selenite concentration. We also tested different exposure durations (50 ppm sodium selenite) and found beta-galactosidase expression peaked at ~60 min, remaining consistent between 60 and 90 min (Fig. 3d). This suggests that the detection of this transgenic strain should be conducted at ~60 min after radiation exposure for the better measurement consistency. However, since sodium selenite was present with the bacteria until the detection, it was yet unclear about the minimum required exposure duration and how long *DRPZ423* takes to respond to DNA damages.

Further characterization involved measuring beta-galactosidase secretion from *DRPZ423* after X-ray irradiation with different

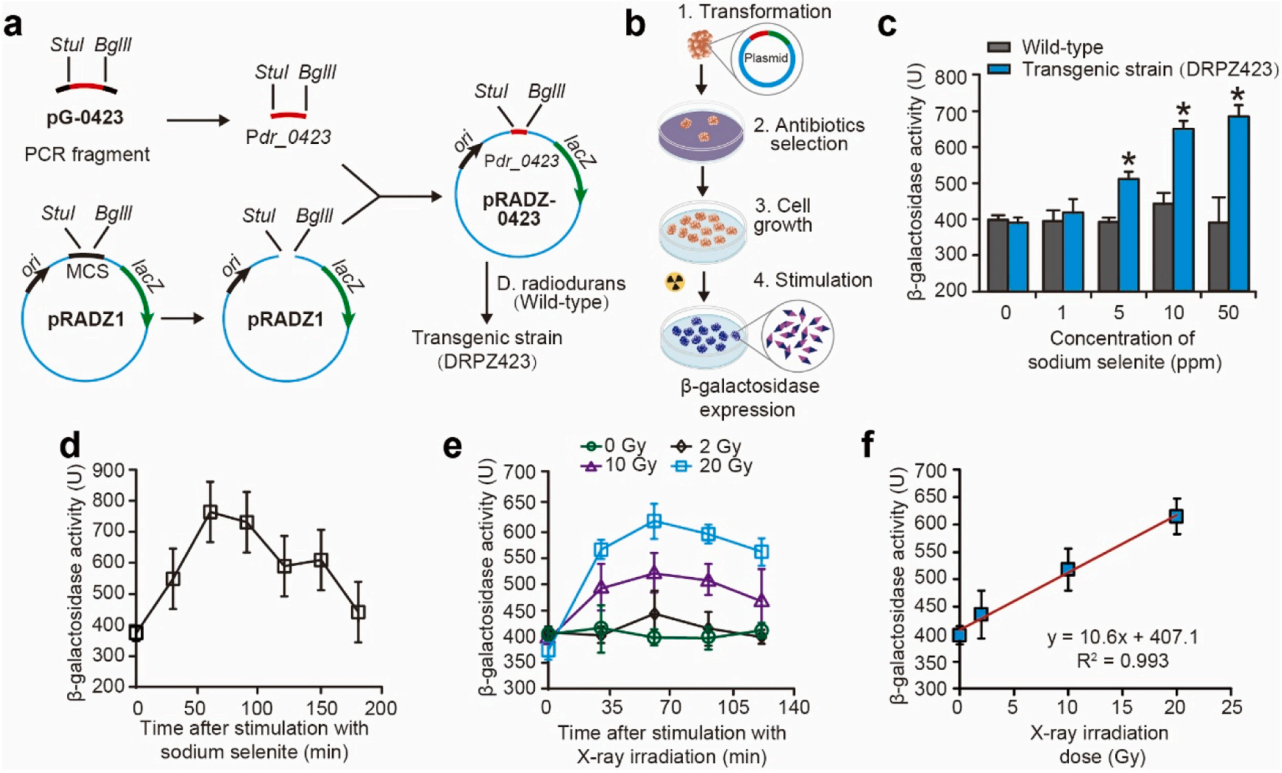

Fig. 3. Generation and evaluation of the genetically modified bacterium *D. radiodurans* (*DRPZ423*). (a) Construction route of plasmid pRADZ-423 and the genetically modified bacterium *D. radiodurans* (*DRPZ423*) for radiation responsive biosensor. ori: origin of replication, lacZ: a gene encodes beta-galactosidase. (b) Schematic of the construction procedures of *DRPZ423*. (c) Activity of beta-galactosidase in transgenic strain *DRPZ423* and wild-type strain exposed to various concentrations of sodium selenite (0 ppm, 1 ppm, 5 ppm, 10 ppm, 50 ppm) for one hour (n = 3). (d) Activity of beta-galactosidase was measured at different time points after adding sodium selenite (50 ppm). (n = 3) (e) Activity of beta-galactosidase was measured at different time points with different doses (0 Gy, 2 Gy, 10 Gy and 20 Gy) of X-ray irradiation (n = 3). (f) The relationship between doses of X-ray and beta-galactosidase expressions (n = 3). Data are presented as mean ± SEM; and asterisks denote significant differences with p-values < 0.05.

subsequent post-exposure time (Fig. 3e) to further characterize the strain. No significant induction of beta-galactosidase occurred right after the irradiation (zero exposure time), but it reached > 90 % of the maximum level by 0.5 h of post-exposure time, peaking at 1 h of post-exposure time and decreasing thereafter (Fig. 3e). Expectedly, the beta-galactosidase level also increased with the doses ranging from 2 Gy to 20 Gy. Such levels for 1 h post-exposure time exhibited a reasonable linearity ($R^2 = 0.993$) with radiation energy (Fig. 3f).

2.4. Characterization of DEP trapping

We developed an on-chip DEP-based cell trapper to concentrate DRPZ423 bacteria (10^6 cells/ml) over an electrode region, enhancing beta-galactosidase secretion and improving current detection under ionizing irradiation. The trapper consists of a pair of wide electrodes (200 μm × 300 μm, center-to-center distance: 0.3 mm) for cell trapping, flanked by narrower electrodes (30 μm × 300 μm, center-to-center distance: 1.17 mm) (Fig. 4a). Wide electrodes were driven by an AC voltage (Vpp: 20 V, 30 kHz) with a 3 V DC offset applied to one electrode, producing a stronger electric field gradient around the upstream electrode ('E2' in Fig. 4b) [58]. COMSOL simulations confirmed that the bacteria, due to their higher relative permittivity compared to the media, moved towards the region with a larger electric field strength (Fig. 4c) [59–61].

We analytically evaluated the required V_{pp} for trapping bacteria against drag (F_d) and shear forces (F_s) in the flow (Fig. 4**d**). (The governing equation and analysis are provided in Supplementary Material.) The DEP force (F_{DEP}) and the resultant friction force (F_f) must be sufficiently large to hold the bacteria. The value of $F_d + F_s - F_f$ as a function of Q and V_{pp} is plotted in Fig. 4**e**. For $V_{pp} = 20$ V, we calculated that $F_d = 7.36$ fN, $F_s = 6.54$ fN, and $F_f = 36.44$ pN, implying the bacteria could maintain on the trapper electrode during the device operation [62,63]. We performed an experiment to verify the DEP-trapping of *DRPZ423* with $V_{pp} = 20$ V and an offset voltage of 3 V that the bacteria (stained with 4'-6-diamidino-2-phenylindole (DAPI), Fig. 4**f**) could be trapped at the trapper electrode (point A of Fig. 4**e** and the left micrograph of Fig. 4**f**), recorded by an inverted microscope (Nikon TE 300, Nikon, Japan) with a SCMOS CCD camera (Zyla 5.5, Andor, UK). Next, the microvalve opened to allow a media flow of ~0.08 nl/min for 3 min; and the bacteria could stay on the trapper electrode (point B of Fig. 4**e** and the middle micrograph of Fig. 4**f**). Once after reducing V_{pp} to 4 V (and the offset voltage scaled accordingly to 0.6 V) such that $F_d + F_s > F_f$ (≈ 7.26 pN), the bacteria were released and escaped from the trapper region (point C of Fig. 4**e** and the right micrograph of Fig. 4**f**).

We investigated whether DEP-induced trapping could cause DNA damage in *DRPZ423*. Bacteria were trapped on the electrode using DEP for two pre-trapping periods (0 h and 0.5 h) before the amperometric detection by balancing capture time, cell viability with experimental throughput. After adding PAPG (1 mM in 1 × phosphate buffered saline) and waiting for 1 min, the media was transferred to the electrochemical detection chamber for current measurement. Our results showed no significant difference in electrical current between the groups, indicating that DEP did not induce notable DNA damage or beta-galactosidase secretion (Fig. 4**g**). Viability tests also showed an insignificant reduction in cell viability due to DEP operation (Fig. 4**h**).

Additionally, we assessed the effects of DEP-trapping on ionizing irradiation measurements. *DRPZ423* bacteria were exposed to alpha-particle irradiation from a ^{241}Am isotope source (5.49 MeV, 4.26 kBq)

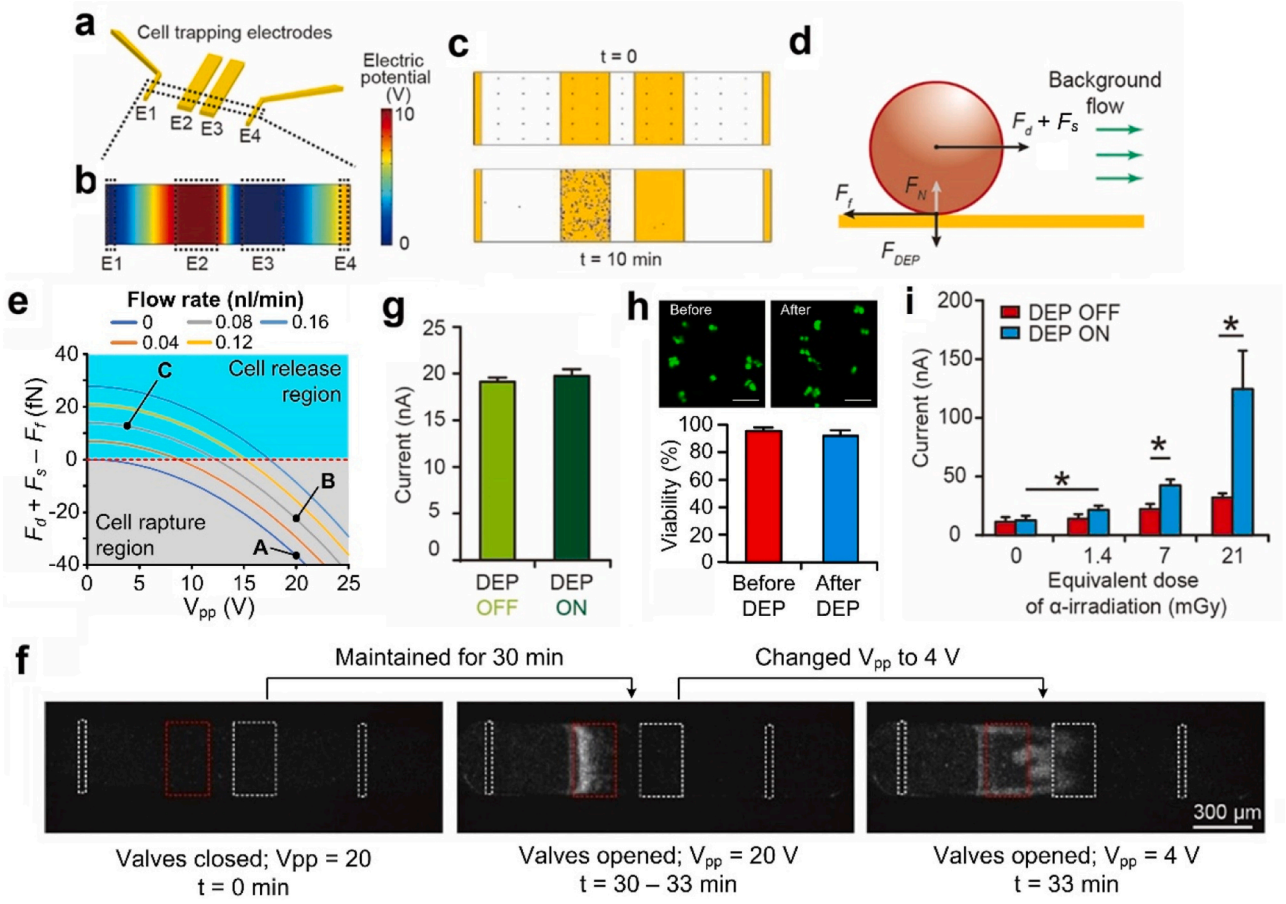

Fig. 4. Experimental and numerical characterization of DEP trapping. (a) Schematic of the cell trapping electrodes (E1, E2, E3 and E4). (b) Simulated potential distribution in the DEP-based cell trapping chamber. (c) Simulated particle trapping performance in the DEP-based cell trapping chamber before (t = 0) and after turning on the electric field gradient for 10 min. (d) Schematic of forces acting on a sphere in contact with a plane surface, used to evaluate the required V_{pp} for holding bacteria under a defined flow rate. Forces include the DEP-induced friction force (F_{DEP}), drag force (F_d), normal force (F_N), and friction force (F_f). (e) Relationship between V_{pp} and $F_d - F_f$ under different flow rates. The dashed line indicates the boundary separating the cell release region (*light cyan*) and the cell capture region (*light gray*). (f) Representative images of experimental bacteria trapping process. (g) Amperometric detection results for samples with/without trapping process. It indicates that no DNA damage and beta-galactosidase secretion will be induced by DEP-based cell trapping (n = 5). (h) Cell viability before and after the DEP-trapping of 30 min. Representative cell-stained micrographs of live (*green*) and dead (*red*) cells before and after the DEP-trapping are also provided (n = 114). Scale bar: 1 μm. (**i**) Effects of DEP-trapping on the measurement of ionizing irradiation toxicity in *DRPZ423* after different doses (1.4 mGy, 7 mGy and 21 mGy) of alpha-particle irradiation using an ^{241}Am isotope (n = 3). Data are presented as mean ± SEM; and asterisks denote significant differences with p-values < 0.05.

at doses of 1.4 mGy, 7 mGy, and 21 mGy.

The measured current levels (Fig. 4**i**) were then obtained with the amperometric detection procedures as above. A stronger current could be measured with DEP. Nonetheless, considering ionizing irradiation induces DNA damage in the nucleus of human cells, the bacteria should be trapped by DEP at the electrode surface for a more representative measurement. The DNA molecules in bacteria could then have a defined distance from the overhead device membrane, geometrically analogous to the distance between nuclear DNAs and the membrane of a target human cell type.

2.5. Characterization of electrochemical detection

We performed experiments to investigate the amperometric detection scheme. After we inserted *DRPZ423* (10^6 cells/ml) in the microfluidic chip, the cells were trapped on the trapper electrode by DEP. Instead of applying ionizing radiation externally, we treated the trapped *DRPZ423* cells with varying concentrations of sodium selenite (0–10 ppm) by injecting it directly into the bacteria trapping chamber. An Emstat3 + potentiostat was applied to measure the required current level, ranging from sub-nanoamperes to milliamperes. Following the amperometric detection procedures, we observed a strong positive correlation ($R^2 = 0.978$) between the sodium selenite concentration and the measured current (Fig. 5**a**). This relationship reflects the correlation between beta-galactosidase activity and the induced current. We performed another experiment to induce the expression of beta-galactosidase by the chemical stimulus with the operation parameters as above to characterize detected current for different reaction time (ranging 1 – 30 min) of PAPG in the radiation detection chamber using the engineered *DRPZ423* cells [64]. The results showed that the signal was stable within 10 min (Fig. 5**b**), indicating the working measurement duration, and gradually decreased afterward.

Furthermore, we examined the effects of the ultra-thin PDMS membrane on the radiation measurement. Among various ionizing irradiations, we chose an alpha radiation source in our test due to the low penetration capability. That is, if there was no significant reduction caused by the PDMS membrane, there should not be a large reduction for other radiation types. We adopted the ^{241}Am isotope as the radiation source for each exposure of 2 min. We then applied the alpha-particle irradiation on a poly allyl diglycol carbonate (PADC) film with and without covered by the microfabricated PDMS membrane (thickness: 1.5 μm). The PADC film functioned as an alpha-particle track detector

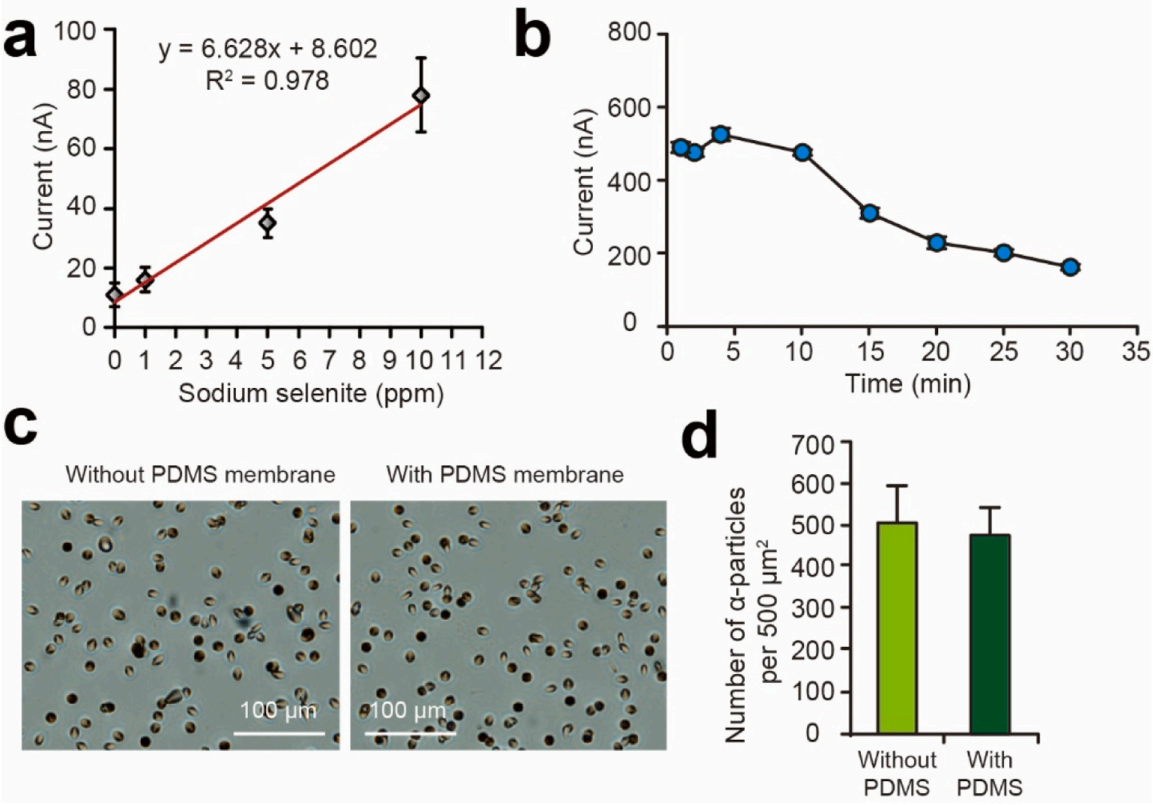

Fig. 5. Characterization of on-chip electrochemical detection. (a) Amperometric detection results for transgenic strain *DRPZ423* exposed to various concentrations of sodium selenite (0 ppm, 1 ppm, 5 ppm, 10 ppm) for 1 h (n = 3). (b) A profile of measured current along the reaction time of PAPG of the stimulated bacteria in the irradiation chamber (n = 3). (c) Tracks of alpha particles passing through the control (without PDMS membrane) and the PDMS membrane-sandwiched poly allyl diglycol carbonate (PADC) films after chemical etching these films. (d) Quantification of the number of alpha particle tracks left on the PADC films after the alpha-particle irradiation with and without the PDMS membrane (n = 20). Data are presented as mean ± SEM.

[65,66] that the exposure of an alpha particle created atomic displacement and molecular rearrangement, which then formed as cylindrical tracks after chemically etched in sodium hydroxide (6.25 mol/l, at 70 °C for 4 h) and imaged by a brightfield microscope. Results (Fig. 5c&d) show no significant difference in the number of alpha-particle tracks caused by coverage of the PDMS membrane, suggesting that the membrane was thin enough to allow the alpha particles, as possibly other radiation with higher penetration capability, to pass through.

2.6. Quantification of ionizing irradiation using the radiation toxicity biosensing platform

We evaluated the sensing performance of the radiation whole-cell biosensing platform for X-ray and alpha radiation applied on top of the PDMS membrane and followed the same procedures as above (Fig. 6**a**). First, we applied X-ray irradiation with different doses (0 – 20 Gy) to the biosensing platform; and the results (Fig. 6**b**) show a linear correlation ($R^2 = 0.919$) between the dose (D_{in}; unit: Gy) and the output current (I_{out}; unit: mA), determined as $I_{out} = 0.17D_{in} + 1.49$. The sensitivity was calculated as 0.17 mA/Gy. The limit of detection was calculated by $3\sigma/S = 318$ mGy, where σ is the standard deviation of the blank sample and S is the slope of the standard curve [67].

Next, we applied alpha-particle irradiation (^{241}Am isotope) with different doses, ranging about 0 – 22 mGy. The measured current gradually increased with a larger dose of alpha radiation (Fig. 6**c**), which was consistent with the previous reports [68]. The linear regression (R^2=0.981) was determined as $I_{out} = 5.4D_{in} + 4.6$; a sensitivity of 5.4 mA/Gy and a limit of detection was 2.40 mGy. Interestingly, the ratios of current / irradiation dose (Fig. 6**d**) demonstrate that alpha particles can cause three orders of magnitude higher DNA damage-induced current than X-ray.

To validate implementation of the reported biosensing platform as a radiation toxicity assay, we conducted a recovery testing with a set of recovered bacteria strains exposed with different alpha irradiation doses (4.67 mGy, 9.33 mGy, and 42 mGy). The bacteria were frozen in liquid nitrogen for three months, followed by resuspension and culturing for four weeks. For each sample, three repeated measurements with the same dose were conducted, with an idle time of 10 min between measurements, to evaluate the relative standard deviation (RSD) derived by multiplying the standard deviation by 100 and dividing the result by the measured average and the recovery rate that was defined as the relative deviation of the measured average from the expected value. Our results (Table S3) show that the recovery rate is > 93.3 % and the RSD is 2.78 – 6.38 %, compared to other reported works. For examples, an RSD of 7 – 30 % was reported in whole-cell bioreporters for the investigation of pollutant bioavailability in water and soil/sediment [69]. An RSD of ~7.8 % was reported in detection of chlorinated and brominated hydrocarbons using an ion sensitive whole cell biosensor [70]. An RSD of 3 – 25 % was reported for a visual whole-cell biosensor toward metal ions in culture medium prepared using environmental water [71]. Overall, our reported biosensing scheme offers a relatively consistent measurement compared to other whole-cell biosensors.

3. Conclusion

We have developed a novel radiation toxicity whole-cell biosensing scheme. We have constructed a transgenic strain *DRPZ423* by cloning our discovered unique radiation-responsive gene *dr_0423* in the radioresistant *D. radiodurans*. Radiation toxicity is measured as the current induced by ionizing irradiation on *DRPZ423* such that the resultant

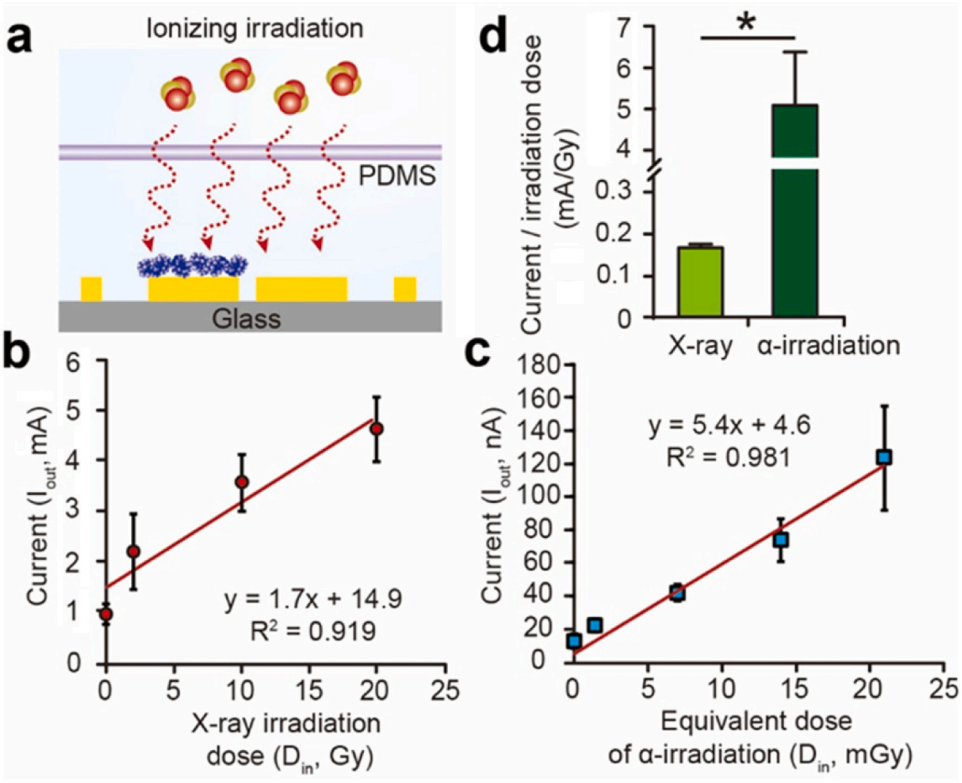

Fig. 6. Quantification of the toxicity of X-ray and alpha radiation using the radiation toxicity biosensor. (a) Schematic of radiation toxicity detection using the PDMS membrane-embedded microfluidic biosensor. (b) Amperometric detection results for *DRPZ423* irradiated by various doses (0 – 20 Gy) of X-ray irradiation. A linear correlation was obtained between the measured current (I_{out}; unit: mA) and the dose (D_{in}; unit: Gy). (n = 3) (c) The relationship of amperometric detection results (I_{out}; unit: nA) and different doses (D_{in}; unit: mGy) of alpha-particle irradiation using a ^{241}Am α-particle source (n = 3). (d) Quantified results of the ratios of measured current over irradiation current with the unit of mA/Gy (n = 3).

secretion of beta-galactosidase catalyzes the conversion of PAPG to PAP compatible with the amperometric detection. *DRPZ423* functions as a key sensing element in a microfluidic chamber having an ultra-thin overhead membrane (1.5 μm thick) for improved specificity. Aided by theoretical studies, DEP with an offset voltage has been successfully implemented to focus *DRPZ423* (10^6 cells) at an electrode (area: 0.06 mm^2) for higher sensitivity. The microstructural design can also achieve an improved recovery rate (>93.30 %) and an RSD (2.78 – 6.38 %) for small volumes (in a sub-microliter scale) of detection samples. This device can also achieve the long-term monitoring of radiation toxicity by regular measurements over time. As radiation toxicity reflects better the potential human health hazards upon irradiation than radiation energy does, which is measured by many physical sensors, this technique can be applied in detecting the bio-hazardous of unknown radioactive contamination in various environmental samples. Given the rapid increments of radioactive waste from industry, medical and scientific research, the reported technique can evaluate the toxicity of unknown radiation-risky samples and defined radiation sources.

CRediT authorship contribution statement

Lam Raymond H. W.: Writing – review & editing, Supervision, Funding acquisition, Conceptualization. **Cui Xin:** Writing – review & editing, Writing – original draft, Formal analysis, Data curation. **Yang Chengpeng:** Writing – original draft, Methodology, Formal analysis, Conceptualization. **Li Vincent W. T.:** Writing – original draft, Validation, Formal analysis, Data curation. **Jiang Zhongning:** Validation, Methodology, Formal analysis. **Marcos:** Methodology, Supervision. **Qu Yun:** Visualization, Validation, Formal analysis. **Yu Peter K. N.:** Software, Resources, Methodology. **Cheng S. H.:** Software, Resources, Methodology. **Huang Siping:** Writing – original draft, Formal analysis. **Yao Xin:** Methodology, Formal analysis. **Lau Cia Hin:** Visualization, Validation, Software.

Declaration of Competing Interest

The authors declare that they have no known competing financial interests or personal relationships that could have appeared to influence the work reported in this paper.

Acknowledgements

This work was supported by Hong Kong Research Grant Council (General Research Grant 11206324 and 11217373).

Appendix A. Supporting information

Supplementary data associated with this article can be found in the online version at doi:10.1016/j.snb.2025.137546.

Data Availability

Data will be made available on request.

References

[1] A.O. Adeola, K.O. Iwuozor, K.G. Akpomie, K.A. Adegoke, K.O. Oyedotun, J. O. Ighalo, J.F. Amaku, C. Olisah, J. Conradie, Advances in the management of radioactive wastes and radionuclide contamination in environmental compartments: a review, Environ. Geochem. Health 45 (2023) 2663–2689, https://doi.org/10.1007/s10653-022-01378-7.

[2] Z. Lin, S. Lv, Z. Yang, J. Qiu, S. Zhou, Structured scintillators for efficient radiation detection, Adv. Sci. 9 (2022) e2102439, https://doi.org/10.1002/advs.202102439.

[3] A. Mishra, H. Siddiqi, B. Meikap, Elucidating sustainable waste management approaches along with waste-to-energy pathways: a critical review, Energy Waste (2022) 83–96, https://doi.org/10.1201/9781003178354-8.

[4] E. Sanganyado, Policies and regulations for the emerging pollutants in freshwater ecosystems: challenges and opportunities, Emerg. Freshw. Pollut. (2022) 361–372, https://doi.org/10.1016/b978-0-12-822850-0.00007-7.

[5] F.M. Adebiyi, O.T. Ore, A.O. Adeola, S.S. Durodola, O.F. Akeremale, K. O. Olubodun, O.K. Akeremale, Occurrence and remediation of naturally occurring radioactive materials in Nigeria: a review, Environ. Chem. Lett. 19 (2021) 3243–3262, https://doi.org/10.1007/s10311-021-01237-4.

[6] J. Sia, R. Szmyd, E. Hau, H.E. Gee, Molecular mechanisms of radiation-induced cancer cell death: a primer, Front. Cell Dev. Biol. 8 (2020) 41, https://doi.org/10.3389/fcell.2020.00041.

[7] I. Publ, 2007 recommendations of the International Commission on Radiological Protection, Ann. Icrp 37 (2008) 2–4, https://www.icrp.org/publication.asp?id=ICRP%20Publication%20103.

[8] N.A. Khan, V. Vambol, S. Vambol, B. Bolibrukh, M. Sillanpaa, F. Changani, A. Esrafili, M. Yousefi, Hospital effluent guidelines and legislation scenario around the globe: a critical review, J. Environ. Chem. Eng. 9 (2021) 105874, https://doi.org/10.1016/j.jece.2021.105874.

[9] J. Guo, Y. Liu, X. Wu, J. Chen, Assessment of the impact of Fukushima nuclear wastewater discharge on the global economy based on GTAP, Ocean Coast. Manag. 228 (2022) 106296, https://doi.org/10.1016/j.ocecoaman.2022.106296.

[10] J. Xie, Y. Wang, W. Liu, X. Yin, L. Chen, Y. Zou, J. Diwu, Z. Chai, T.E. Albrecht-Schmitt, G. Liu, Highly sensitive detection of ionizing radiations by a photoluminescent uranyl organic framework, Angew. Chem. 129 (2017) 7608–7612, https://doi.org/10.1002/ange.201700919.

[11] M.I. Ahmad, M.H. Ab. Rahim, R. Nordin, F. Mohamed, A. Abu-Samah, N. F. Abdullah, Ionizing radiation monitoring technology at the verge of internet of things, Sensors 21 (2021) 7629, https://doi.org/10.3390/s21227629.

[12] A. Kulkarni, B. Kim, S.R. Dugasani, P. Joshirao, J.A. Kim, C. Vyas, V. Manchanda, T. Kim, S.H. Park, A novel nanometric DNA thin film as a sensor for alpha radiation, Sci. Rep. 3 (2013) 2062.

[13] M.P. Taggart, M.D. Tarn, M.M. Esfahani, D.M. Schofield, N.J. Brown, S. J. Archibald, T. Deakin, N. Pamme, L.F. Thompson, Development of radiodetection systems towards miniaturised quality control of PET and SPECT radiopharmaceuticals, Lab a Chip 16 (2016) 1605–1616, https://doi.org/10.1039/c6lc00099a.

[14] J. Jones, N.S. Ha, A.G. Barajas, A.F. Chatziioannou, R.M. van Dam, Integration of high-resolution radiation detector for hybrid microchip electrophoresis, Anal. Chem. 92 (2020) 3483–3491, https://doi.org/10.1021/acs.analchem.9b04827.

[15] J.S. Cho, R. Taschereau, S. Olma, K. Liu, Y.-C. Chen, C.K. Shen, R.M. Van Dam, A. F. Chatziioannou, Cerenkov radiation imaging as a method for quantitative measurements of beta particles in a microfluidic chip, Phys. Med. Biol. 54 (2009) 6757, https://doi.org/10.1088/0031-9155/54/22/001.

[16] U. Rössler, S. Hornhardt, C. Seidl, E. Müller-Laue, L. Walsh, W. Panzer, E. Schmid, R. Senekowitsch-Schmidtke, M. Gomolka, The sensitivity of the alkaline comet assay in detecting DNA lesions induced by X rays, gamma rays and alpha particles, Radiat. Prot. Dosim. 122 (2006) 154–159, https://doi.org/10.1093/rpd/ncl424.

[17] R. Sahani, A. Dixit, A comprehensive review on zinc oxide bulk and nano-structured materials for ionizing radiation detection and measurement applications, Mater. Sci. Semicond. Process. 151 (2022) 107040, https://doi.org/10.1016/j.mssp.2022.107040.

[18] S.R. Santa Maria, D.B. Marina, S. Massaro Tieze, L.C. Liddell, S. Bhattacharya, BioSentinel: long-term saccharomyces cerevisiae preservation for a deep space biosensor mission, Astrobiology 23 (2023) 617–630, https://doi.org/10.1089/ast.2019.2073.

[19] Y. Inaba, K. Chida, Y. Murabayashi, M. Endo, K. Otomo, M. Zuguchi, An initial investigation of a wireless patient radiation dosimeter for use in interventional radiology, Radiol. Phys. Technol. 13 (2020) 321–326, https://doi.org/10.1007/s12194-020-00575-2.

[20] Y. Guo, D.L. Zhu, M.Q. Liu, Y.T. Chen, S.Y. Hu, C.Y. Hui, Metabolic engineering-enabled dual-color biosensor for discriminative and sensitive detection of toxic lead and mercury in environmental waters, J. Environ. Chem. Eng. 12 (2024), https://doi.org/10.1016/j.jece.2024.114178.

[21] X.K. Zhang, B.L. Li, D.N. Schillereff, R.C. Chiverrell, B. Tefsen, M. Wells, Whole-cell biosensors for determination of bioavailable pollutants in soils and sediments: theory and practice, Sci. Total Environ. 811 (2022), https://doi.org/10.1016/j.scitotenv.2021.152178.

[22] R. Ramos, A. Karaiskou, C. Botuha, S. Amhaz, M. Trichet, F. Dingli, J. Forte, F. Lam, A. Canette, C. Chaumeton, M. Salome, T. Chenuel, C. Bergonzi, P. Meyer, S. Bohic, D. Loew, M. Salmain, J. Sobczak-Thepot, Identification of cellular protein targets of a half-Sandwich iridium(III) complex reveals its dual mechanism of action via both electrophilic and oxidative stresses, J. Med. Chem. 67 (2024) 6189–6206, https://doi.org/10.1021/acs.jmedchem.3c02000.

[23] J.M. Hernández-Sancho, A. Boudigou, M.V.G. Alván-Vargas, D. Freund, J.A. Bååth, P. Westh, K. Jensen, L. Noda-García, D.C. Volke, P.I. Nikel, A versatile microbial platform as a tunable whole-cell chemical sensor, Nat. Commun. 15 (2024), https://doi.org/10.1038/s41467-024-52755-y.

[24] C.J. Liu, H. Yu, B.C. Zhang, S.L. Liu, C.G. Liu, F. Li, H. Song, Engineering whole-cell microbial biosensors: design principles and applications in monitoring and treatment of heavy metals and organic pollutants, Biotechnol. Adv. 60 (2022), https://doi.org/10.1016/j.biotechadv.2022.108019.

[25] A.S.G. Mendoza, M.F.M. Acosta, J.A.M. Sanchez, L.E.C. Vazquez, Principles and challenges of whole cell microbial biosensors in the food industry, J. Food Sci. 89 (2024) 5255–5269, https://doi.org/10.1111/1750-3841.17294.

[26] M. Moraskie, M.H.O. Roshid, G. O'Connor, E. Dikici, J.-M. Zingg, S. Deo, S. Daunert, Microbial whole-cell biosensors: current applications, challenges, and future perspectives, Biosens. Bioelectron. 191 (2021) 113359, https://doi.org/10.1016/j.bios.2021.113359.

[27] M.O. Elasri, R.V. Miller, Study of the response of a biofilm bacterial community to UV radiation, Appl. Environ. Microbiol. 65 (1999) 2025–2031, https://doi.org/10.1128/aem.65.5.2025-2031.1999.

[28] M. Elasri, R. Miller, A Pseudomonas aeruginosa biosensor responds to exposure to ultraviolet radiation, Appl. Microbiol. Biotechnol. 50 (1998) 455–458, https://doi.org/10.1007/s002530051320.

[29] J. Min, C.W. Lee, S.-H. Moon, R.A. LaRossa, M.B. Gu, Detection of radiation effects using recombinant bioluminescent Escherichia coli strains, Radiat. Environ. Biophys. 39 (2000) 41–45, https://doi.org/10.1007/pl00007683.

[30] Z. Liu, X. Lan, Microfluidic radiobioassays: a radiometric detection tool for understanding cellular physiology and pharmacokinetics, Lab a chip 19 (2019) 2315–2339, https://doi.org/10.1039/c9lc00159j.

[31] Z. Ma, J. Liu, J.B. Sallach, X. Hu, Y. Gao, Whole-cell paper strip biosensors to semi-quantify tetracycline antibiotics in environmental matrices, Biosens. Bioelectron. 168 (2020) 112528, https://doi.org/10.1016/j.bios.2020.112528.

[32] M. Guo, J. Wang, R. Du, Y. Liu, J. Chi, X. He, K. Huang, Y. Luo, W. Xu, A test strip platform based on a whole-cell microbial biosensor for simultaneous on-site detection of total inorganic mercury pollutants in cosmetics without the need for predigestion, Biosens. Bioelectron. 150 (2020) 111899, https://doi.org/10.1016/j.bios.2019.111899.

[33] S.Y. Chen, Y. Zhang, R. Li, B. Wang, B.C. Ye, De Novo design of the ArsR regulated P(ars) promoter enables a highly sensitive whole-cell biosensor for arsenic contamination, Anal. Chem. 94 (2022) 7210–7218, https://doi.org/10.1021/acs.analchem.2c00055.s001.

[34] X. Zhu, G. Wu, Y. Xing, C. Wang, X. Yuan, B. Li, Evaluation of single and combined toxicity of bisphenol A and its analogues using a highly-sensitive micro-biosensor, J. Hazard Mater. 381 (2020) 120908, https://doi.org/10.1016/j.jhazmat.2019.120908.

[35] X. Cui, L. Liu, J. Li, Y. Liu, Y. Liu, D. Hu, R. Zhang, S. Huang, Z. Jiang, Y. Wang, A microfluidic platform revealing interactions between leukocytes and cancer cells on topographic micropatterns, Biosensors 12 (2022) 963, https://doi.org/10.3390/bios12110963.

[36] L.W. Hsu, Y.H. Lin, J.Y. Guo, C.F. Chen, Y.J. Chou, Y.C. Yeh, Simultaneous determination of l-phenylalanine, phenylethylamine, and phenylacetic acid using three-color whole-cell biosensors within a microchannel device, ACS Appl. Bio Mater. 3 (2020) 5120–5125, https://doi.org/10.1021/acsabm.0c00590.s001.

[37] S. Han, Q. Zhang, X. Zhang, X. Liu, L. Lu, J. Wei, Y. Li, Y. Wang, G. Zheng, A digital microfluidic diluter-based microalgal motion biosensor for marine pollution monitoring, Biosens. Bioelectron. 143 (2019) 111597, https://doi.org/10.1016/j.bios.2019.111597.

[38] J. Wang, W. Song, Y. Song, D. Xu, M. Zhang, X. Pan, Y. Sun, D. Li, Quantitative evaluation of radiation dose by γ-H2AX on a microfluidic chip in a miniature fluorescence cytometer, Radiat. Meas. 62 (2014) 71–77, https://doi.org/10.1016/j.radmeas.2014.01.007.

[39] N. Kumar, W. Wang, J.C. Ortiz-Marquez, M. Catalano, M. Gray, N. Biglari, K. Hikari, X. Ling, J. Gao, T. van Opijnen, K.S. Burch, Dielectrophoresis assisted rapid, selective and single cell detection of antibiotic resistant bacteria with G-FETs, Biosens. Bioelectron. 156 (2020) 112123, https://doi.org/10.1016/j.bios.2020.112123.

[40] R.H. Lam, X. Cui, W. Guo, T. Thorsen, High-throughput dental biofilm growth analysis for multiparametric microenvironmental biochemical conditions using microfluidics, Lab a chip 16 (2016) 1652–1662, https://doi.org/10.1039/c6lc00072j.

[41] C.-H. Chiou, L.-J. Chien, T.-C. Chou, J.-L. Lin, J.T. Tseng, Rapid whole-cell sensing chip for low-level arsenite detection, Biosens. Bioelectron. 26 (2011) 2484–2488, https://doi.org/10.1016/j.bios.2010.10.037.

[42] M. S, A.I. Brown, E.F. Koslover, Getting around the cell: physical transport in the intracellular world, Phys. Biol. 17 (2020) 061003, https://doi.org/10.1088/1478-3975/aba5e5.

[43] I.V. Mavragani, Z. Nikitaki, S.A. Kalospyros, A.G. Georgakilas, Ionizing radiation and complex DNA damage: from prediction to detection challenges and biological significance, Cancers 11 (2019), https://doi.org/10.3390/cancers11111789.

[44] M. Liu, Q. Liu, Q. Zou, J. Li, Z. Chu, J. Xiang, W.Q. Chen, Z.F. Miao, B. Wang, The composition and roles of gastric stem cells in epithelial homeostasis, regeneration, and tumorigenesis, Cell. Oncol. (2023), https://doi.org/10.1007/s13402-023-00802-z.

[45] T. Kumagai, F. Rahman, A.M. Smith, The microbiome and radiation induced-bowel injury: evidence for potential mechanistic role in disease pathogenesis, Nutrients 10 (2018), https://doi.org/10.3390/nu10101405.

[46] A.J. Crompton, K.A. Gamage, A. Jenkins, C.J. Taylor, Alpha particle detection using alpha-induced air radioluminescence: a review and future prospects for preliminary radiological characterisation for nuclear facilities decommissioning, Sensors 18 (2018) 1015, https://doi.org/10.3390/s18041015.

[47] E.A. Kwizera, M. Sun, A.M. White, J. Li, X. He, Methods of generating dielectrophoretic force for microfluidic manipulation of bioparticles, ACS Biomater. Sci. Eng. 7 (2021) 2043–2063, https://doi.org/10.1021/acsbiomaterials.1c00083.

[48] K. Selvam, J.R. Duncan, M. Tanaka, J.R. Battista, DdrA, DdrD, and PprA: components of UV and mitomycin C resistance in Deinococcus radiodurans R1, PLoS One 8 (2013) e69007, https://doi.org/10.1371/journal.pone.0069007.

[49] D. Slade, M. Radman, Oxidative stress resistance in Deinococcus radiodurans, Microbiol. Mol. Biol. Rev. MMBR 75 (2011) 133–191, https://doi.org/10.1128/MMBR.00015-10.
[50] G. GuanJun, F. Lu, L. HuiMing, H. YueJin, Engineering Deinococcus radiodurans into biosensor to monitor radioactivity and genotoxicity in environment, Chin. Sci. Bull. 53 (2008) 1675–1681, https://doi.org/10.1007/s11434-008-0224-6.
[51] H. Luan, N. Meng, J. Fu, X. Chen, X. Xu, Q. Feng, H. Jiang, J. Dai, X. Yuan, Y. Lu, A. A. Roberts, X. Luo, M. Chen, S. Xu, J. Li, C.J. Hamilton, C. Fang, J. Wang, Genome-wide transcriptome and antioxidant analyses on gamma-irradiated phases of deinococcus radiodurans R1, PLoS One 9 (2014) e85649, https://doi.org/10.1371/journal.pone.0085649.
[52] Y. Liu, J. Zhou, M.V. Omelchenko, A.S. Beliaev, A. Venkateswaran, J. Stair, L. Wu, D.K. Thompson, D. Xu, I.B. Rogozin, E.K. Gaidamakova, M. Zhai, K.S. Makarova, E. V. Koonin, M.J. Daly, Transcriptome dynamics of Deinococcus radiodurans recovering from ionizing radiation, Proc. Natl. Acad. Sci. USA 100 (2003) 4191–4196, https://doi.org/10.1073/pnas.0630387100.
[53] D.J. Rocha, C.S. Santos, L.G. Pacheco, Bacterial reference genes for gene expression studies by RT-qPCR: survey and analysis, Antonie Van. Leeuwenhoek 108 (2015) 685–693, https://doi.org/10.1007/s10482-015-0524-1.
[54] X. Dai, Y. Li, R. Zhang, Y. Kou, X. Mo, J. Cao, Y. Xiong, Effects of sodium selenite on c-Jun N-terminal kinase signalling pathway induced by oxidative stress in human chondrocytes and c-Jun N-terminal kinase expression in patients with Kashin-Beck disease, an endemic osteoarthritis, Br. J. Nutr. 115 (2016) 1547–1555, https://doi.org/10.1017/s0007114516000362.
[55] D.R. Harris, M. Tanaka, S.V. Saveliev, E. Jolivet, A.M. Earl, M.M. Cox, J.R. Battista, Preserving genome integrity: the DdrA protein of Deinococcus radiodurans R1, PLoS Biol. 2 (2004) e304, https://doi.org/10.1371/journal.pbio.0020304.
[56] F. Fan, L. Zhang, X. Zhou, F. Mu, G. Shi, A sensitive fluorescent probe for beta-galactosidase activity detection and application in ovarian tumor imaging, J. Mater. Chem. B 9 (2021) 170–175, https://doi.org/10.1039/d0tb02269a.
[57] R. Meima, M.E. Lidstrom, Characterization of the minimal replicon of a cryptic Deinococcus radiodurans SARK plasmid and development of versatile Escherichia coli-D. radiodurans shuttle vectors, Appl. Environ. Microbiol. 66 (2000) 3856–3867, https://doi.org/10.1128/aem.66.9.3856-3867.2000.
[58] N. Mittal, A. Rosenthal, J. Voldman, nDEP microwells for single-cell patterning in physiological media, Lab a chip 7 (2007) 1146–1153, https://doi.org/10.1039/b706342c.
[59] W. Bai, K. Zhao, K. Asami, Dielectric properties of E. coli cell as simulated by the three-shell spheroidal model, Biophys. Chem. 122 (2006) 136–142, https://doi.org/10.1016/j.bpc.2006.03.004.
[60] R. Sender, S. Fuchs, R. Milo, Revised estimates for the number of human and bacteria cells in the body, PLoS Biol. 14 (2016) e1002533, https://doi.org/10.1371/journal.pbio.1002533.
[61] Y. Huang, X.-B. Wang, F.F. Becker, P. Gascoyne, Introducing dielectrophoresis as a new force field for field-flow fractionation, Biophys. J. 73 (1997) 1118–1129, https://doi.org/10.1016/s0006-3495(97)78144-x.
[62] K. Miyoshi, T. Spalvins, and D.H. Buckley, Friction and hardness of gold films deposited by ion plating and evaporation, 1983, ⟨https://ntrs.nasa.gov/citations/19830025748⟩.
[63] C. Lyu, J. Wang, M. Powell-Palm, B. Rubinsky, Simultaneous electroporation and dielectrophoresis in non-electrolytic micro/nano-electroporation, Sci. Rep. 8 (2018), https://doi.org/10.1038/s41598-018-20535-6.
[64] A. Hosseini, J. Mas, The β-galactosidase assay in perspective: critical thoughts for biosensor development, Anal. Biochem. 635 (2021) 114446, https://doi.org/10.1016/j.ab.2021.114446.
[65] S. Guo, B. Chen, S. Durrani, Solid-state nuclear track detectors. Handbook of Radioactivity Analysis, Elsevier, 2020, pp. 307–407, https://doi.org/10.1016/c2016-0-04811-8.
[66] D.G. Naik, V.S. Nadkarni, Poly (triallyl phosphate) and its copolymers with allyl diglycol carbonate as solid state nuclear track detectors, Des. Monomers Polym. 19 (2016) 643–649, https://doi.org/10.1080/15685551.2016.1187445.
[67] A.F. Zhu, S. Ali, Y. Xu, Q. Ouyang, Q.S. Chen, A SERS aptasensor based on AuNPs functionalized PDMS film for selective and sensitive detection of Staphylococcus aureus, Biosens. Bioelectron. 172 (2021), https://doi.org/10.1016/j.bios.2020.112806.
[68] A. Kulkarni, B. Kim, S.R. Dugasani, P. Joshirao, J.A. Kim, C. Vyas, V. Manchanda, T. Kim, S.H. Park, A novel nanometric DNA thin film as a sensor for alpha radiation, Sci. Rep. 3 (2013), https://doi.org/10.1038/srep02062.
[69] X. Zhang, B. Li, D.N. Schillereff, R.C. Chiverrell, B. Tefsen, M. Wells, Whole-cell biosensors for determination of bioavailable pollutants in soils and sediments: theory and practice, Sci. Total Environ. 811 (2022) 152178, https://doi.org/10.1016/j.scitotenv.2021.152178.
[70] J. Peter, W. Hutter, W. Stöllnberger, W. Hampel, Detection of chlorinated and brominated hydrocarbons by an ion sensitive whole cell biosensor, Biosens. Bioelectron. 11 (1996) 1215–1219, https://doi.org/10.1016/0956-5663(96)88086-9.
[71] C. Hui, Y. Guo, L. Li, L. Liu, Y. Chen, J. Yi, N. Zhang, Indigoidine biosynthesis triggered by the heavy metal-responsive transcription regulator: a visual whole-cell biosensor, Appl. Microbiol. Biotechnol. 105 (2021) 6087–6102, https://doi.org/10.1007/s00253-021-11441-5.

Xin Cui received the PhD degree of Mechanical and Biomedical Engineering from City University of Hong Kong, China. Now, he is an Associate Professor in Department of Biomedical Engineering, Jinan University, China, and mainly interested in the research of functional biomaterials-based microfluidics and biosensors.

Chengpeng Yang received the PhD degree of Mechanical and Biomedical Engineering from City University of Hong Kong, China, and interested in developing active mixers and electrical microfluidic biosensors.

Vincent W. T. Li received the PhD degree of Mechanical and Biomedical Engineering from City University of Hong Kong, China, and interested in cell engineering and zebrafish-depended biosensor development.

Siping Huang is a PhD student in Department of Mechanical and Biomedical Engineering at City University of Hong Kong, China, and interested in micro-engineered cell-pairing and microfluidics.

Xin Yao is a Postdoctoral Fellow of Materials Science and Engineering, Nanyang Technological University, Singapore, and interested in energy material, water-splitting.

Cia Hin Laub received the PhD degree of Mechanical and Biomedical Engineering from City University of Hong Kong, China, and interested in targeted transcriptional activation using capsid-modified AAV and CRISPRa.

Zhongning Jiang is a PhD student in Department of Mechanical and Biomedical Engineering at City University of Hong Kong, China, and interested in using microfluidic platforms for investigating immune inter and intra-cellular interactions.

Yun Qu is a PhD student in Department of Mechanical and Biomedical Engineering at City University of Hong Kong, China, and interested in developing biodegradable microrobots for drug delivery.

Marcos is an Associate Professor at School of Mechanical & Aerospace Engineering, Nanyang Technological University, Singapore, and interested in manipulation and sorting of micro-organisms by electrophoretic motion.

Peter K. N. Yu is a Professor at Department of Physics, City University of Hong Kong, Hong Kong, China, and interested in radiation physics, medical physics, radiation biology, radioecology and environmental modeling.

S. H. Cheng is a Chair Professor of Molecular Medicine in the Department of Biomedical Sciences at City University of Hong Kong, China, and interested in how molecules and chemicals interact in regulating the embryonic development and adult organ regeneration.

Raymond H. W. Lam is an Associate Professor in the Department of Mechanical and Biomedical Engineering at City University of Hong Kong, China, and interested in cell mechanobiology, bacteriology, microfluidics, microfabrication and computational methods.